Theory of the neutral nitrogen-vacancy center in diamond and its application to the realization of a qubit

Adam Gali
Department of Atomic Physics, Budapest University of Technology and Economics, Budafoki út 8, H-1111 Budapest, Hungary
(Received 5 January 2009; revised manuscript received 26 May 2009; published 30 June 2009)

The negatively charged nitrogen-vacancy defect (NV^-) in diamond has attracted much attention in recent years in qubit and biological applications. The negative charge is donated from nearby nitrogen donors that could limit or stem the successful application of NV^-. In this study, we identify the *neutral* nitrogen-vacancy defect (NV^0) by *ab initio* supercell calculations through the comparison of the measured and calculated hyperfine tensors of the $^4A_2$ excited state. Our analysis shows that (i) the spin state can be *selectively* occupied optically, (ii) the electron spin state can be manipulated by time-varying magnetic field, and (iii) the spin state may be read out optically. Based on this NV^0 is a hope for realizing qubit in diamond *without* the need of nitrogen donors. In addition, we propose that NV^0 may be more sensitive magnetometer than the ultrasensitive NV^-.

DOI: 10.1103/PhysRevB.79.235210 PACS number(s): 71.15.Mb, 61.72.Bb, 71.55.Ht

I. INTRODUCTION

Realization of qubits is of extremely high importance because that can be used in quantum cryptography, quantum optics, and quantum computing. One of the most promising candidates is the *negatively charged* nitrogen-vacancy defect (NV^-) (Refs. 1 and 2) that can operate at *room temperature*.[3–11] The negative charge is donated from nitrogen substitutional (N_S).[12,13] It has been very recently shown that the major source of the decoherence of the electron spin of the negatively charged NV center is the electron spin bath of nitrogen substitutionals in type-*Ib* diamond, that can be eliminated only at low temperature using a giant magnetic field.[14] This is a serious limiting factor toward the development for *practical* applications. In addition, it has been recently demonstrated that nanometer-sized diamond particles containing NV^- are useful as fluorescent biomarkers for *in vitro* imaging applications.[15,16] However, the requirement of the extra charge on NV defect from N_S could be critical in biomarker applications, where the size of the nanodiamond is reduced to some nanometers in diameter.[17] One solution of this problem would be to apply the paramagnetic *neutral* NV defect (NV^0) which produces strong photoluminescence (PL) at 2.156 eV (similar to NV^-) and it *does not require an extra electron*. The NV^- center is well identified[12] while its strong connection to its neutral counterpart is well established experimentally.[18–20] However, the overall knowledge about NV^0 is scarce. Very recently, an $S=\frac{3}{2}$ electron-paramagnetic-resonance (EPR) center has been found in photoexcited diamond doped by ^{15}N.[21] Sizeable ^{15}N hyperfine constants have been detected in the EPR measurements and it was proposed that the signal was originated from one of the excited states of NV^0.[21] We emphasize that the identification of the EPR signal of NV^0 is a *key step* in order to apply it for qubit and to trace it magnetically in biomarker applications.

In this study we (i) *identify* the EPR signal of NV^0, (ii) provide a detailed spin-density distribution around the defect; the results indicate that the defect states are well localized and the electron spin can be decoupled from the spin bath of ^{13}C nuclei, (iii) analyze the electronic structure by group theory explaining the photoexcitation of NV^0; this shows that the $M_S=\pm 1/2$ sublevels are *selectively* occupied in the photoionization process and appropriate microwave magnetic field can be applied to choose also selectively either $M_S=+3/2$ or $M_S=-3/2$ which finally can be used as qubit, and (iv) we propose that the $M_S=+3/2$ or $M_S=-3/2$ states may be read out optically during the emission process from the excited state to the ground state. This gives a hope for realization of qubit by NV^0 defect. In addition, we have very recently realized that NV^--contained nanodiamonds have been demonstrated to act as ultrasensitive magnetometers.[22,23] Since the sensitivity is proportional to the spin state the $S=3/2$ excited state of the NV^0 defect would suggest an even more sensitive magnetometer than NV^- defect with $S=1$ state.

In the followings we describe briefly our applied computational methodology in Sec. II. We discuss the electronic states of NV^0 in Sec. III then we provide the results obtained by our calculations in Sec. IV. We discuss the possible role of NV^0 defect in spintronics in Sec. V and finally we summarize our results in Sec. VI.

II. COMPUTATIONAL METHODOLOGY

We employed density-functional-theory calculations with local spin-density approximation (LSDA) using a large, 512-atom simple cubic diamond supercell. We used two different codes: the geometry of the defect was optimized with the VASP code[24] while the hyperfine tensors of NV^0 were provided and calculated by the CPPAW code.[25] Both VASP and CPPAW codes apply the all-electron projector augmented-wave method[26] and plane-wave basis set. We used a cutoff of 30 Ry and Γ point for k-point sampling in both codes. Other details and references can be found in our previous publication[27] where we could successfully describe the negatively charged NV center and can predict well the experimental hyperfine data.[28]

III. ELECTRONIC STATES OF THE NV^0 DEFECT IN DIAMOND

The NV defect has C_{3v} symmetry, if no reconstruction occurs. A group-theory analysis based on a single-particle

picture can be very useful in understanding the nature of the defect states and the possible optical transitions between them. As was discussed for the NV^- center previously[27,29–31] four dangling bonds point to the vacant site resulting in the following canonical orbitals:

$$a_1(1):\phi_1 = \sqrt{1-\alpha^2}\sigma_4 - \frac{\alpha}{\sqrt{3}}(\sigma_1+\sigma_2+\sigma_3),$$

$$a_1(2):\phi_2 = \alpha\sigma_4 + \sqrt{\frac{1-\alpha^2}{3}}(\sigma_1+\sigma_2+\sigma_3),$$

$$e_x:\phi_3 = \frac{1}{\sqrt{6}}(2\sigma_1-\sigma_2-\sigma_3),$$

$$e_y:\phi_4 = \frac{1}{\sqrt{2}}(\sigma_2-\sigma_3), \quad (1)$$

where σ_4 is the dangling bond of nitrogen, σ_{1-3} are the dangling bonds of the three C atoms near the vacant site, and $0 \leq \alpha \leq 1$ is a parameter that determines the extent to which the nitrogen dangling bond is mixed in the ϕ_1 and ϕ_2 defect states. According to the calculations ϕ_1 lies deep in energy in the valence band while ϕ_2 and the double degenerate $\phi_{3,4}$ appear in the fundamental band gap. In the case of neutral defect 5 electrons occupy these states. In the ground state ϕ_1 and ϕ_2 defect states are fully occupied while a single electron occupies the double degenerate e level, resulting in $a_1(1)^2a_1(2)^2e^1$ configuration. In this configuration, the system is basically Jahn-Teller unstable because the degenerate e state is only partially filled by electrons. The static Jahn-Teller effect would result in C_{1h} symmetry of the defect. PL studies indicate that the system has C_{3v} symmetry (^2E state) with possibly exhibiting dynamic Jahn-Teller effect that inhibits the EPR detection of the ^2E ground state.[32] We argue that C_{1h} symmetry configuration and the ^2E ground state of C_{3v} symmetry can be described by single Slater determinants, so we could address this issue directly at LSDA level. It may be not trivial that ^2E ground state is from single Slater-determinants. Thus, we analyze further the ^2E ground state. The unpaired electron can either occupy e_x or e_y states in the $a_1(1)^2a_1(2)^2e^1$ configuration. By using the projection operator

$$P^{(j)} = l_j/h\sum_R \chi^j(R)^* P_R,$$

where l_j is the degree of the representation, h is the number of elements in the C_{3v} group, $\chi(R)$ is the character for operation R, and P_R is the symmetry operation R, it is easy to see that single Slater determinants $E_x=a_1(1)^2a_1(2)^2e_x^1$ and $E_y=a_1(1)^2a_1(2)^2e_y^1$ are true and orthonormal eigenstates of the double-degenerate $E=(E_x;E_y)$ ground state in C_{3v} symmetry. The lowest excitation can be obtained by promoting one electron from $a_1(2)$ level to e level resulting in $a_1(1)^2a_1(2)^1e^2$ configuration. The possible excited states of $a_1(1)^2a_1(2)^1e^2$ configuration have $^2A_1$, $^4A_2$, and ^2E multiplets. The $M_S=\frac{3}{2}$ state of $^4A_2$ multiplet can be described by a single Slater-determinant by simply aligning all the electrons spin up on the $a_1(2)$ and e levels, thus the spin density can be determined by usual LSDA calculation. We note that no Jahn-Teller effect occurs for $^4A_2$ state, so we considered only C_{3v} symmetry for this state in the calculations. We focused our research on the ground state of C_{1h} and C_{3v} symmetries, and the $^4A_2$ excited state that are relevant in the recent EPR study.[21] We note here that the nitrogen dangling bond is hybridized into $a_1(2)$ but not into the e defect states, therefore, negligible spin density is expected for the ^2E ground state but considerable spin polarization may be expected for the $^4A_2$ excited state (see Fig. 1). This adjusts the analysis of Felton and co-workers[21] because the possible hybridization of *both* a_1 defect states were not taken into account by them (cf. Refs. 27, 29, and 30). Actually, the calculations already revealed for the negatively charged NV defect that the nitrogen dangling bond hybridizes almost equally both in $a_1(2):\phi_2$ and $a_1(1):\phi_1$ states.[27]

IV. COMPUTED GEOMETRY, ELECTRONIC LEVELS AND HYPERFINE TENSORS

First, we investigated the ground state of NV^0. Since Jahn-Teller effect can occur, we distorted the symmetry to C_{1h} and allowed the atoms to relax to find the energy minimum within LSDA. We found that the system conserves its C_{1h} symmetry and it does not form the C_{3v} configuration. The single occupied e level in the gap is split by 0.3 eV resulting in an occupied a' state and an unoccupied a' state of the spin-up electrons. The neighbor N and C atoms relaxed outward from the vacant site (see Table I). The nitrogen atom remained very close to the $\langle 111 \rangle$ axis even in C_{1h} symmetry while one of the carbon atoms is considerably closer to the vacant site than the other two. Next, we constrained the system to preserve the C_{3v} symmetry during the geometry optimization in order to calculate the total energy of the ^2E state. We found that it is about 0.09 eV higher in energy than the Jahn-Teller distorted one. Then, we allowed the system to relax without symmetry constraints starting from the optimum C_{3v} geometry. The atoms automatically relaxed to the C_{1h} symmetry. This result indicates that C_{3v} symmetry is a saddle point. This finding seems to contradict the PL spectrum which shows ^2E ground state within C_{3v} symmetry. One may argue that LSDA cannot accurately describe the ^2E ground state due to the strong correlation with the ^2E excited states that may lower the energy of the ^2E ground state. While the possibly strong correlation would be effective both for C_{3v} and C_{1h} configurations, this might change the energy hierarchy of the C_{1h} and C_{3v} configurations. The correlation between the ^2E states can be described by advanced configurational-interaction (CI) theory within Hartree-Fock (HF) approximation. We note that the neutral NV defect has been recently investigated in small nanodiamonds by applying HF-CI approximations[33] and they found the C_{1h} symmetry lowest in energy. This result supports our LSDA calculation. We also note that LSDA tends to underestimate the barrier energy, i.e., the total energy of the C_{3v} configuration. These two effects can cancel each other, at least partially. We conclude that the C_{1h} configuration is the static ground state of the NV^0 defect at 0 K and the migration

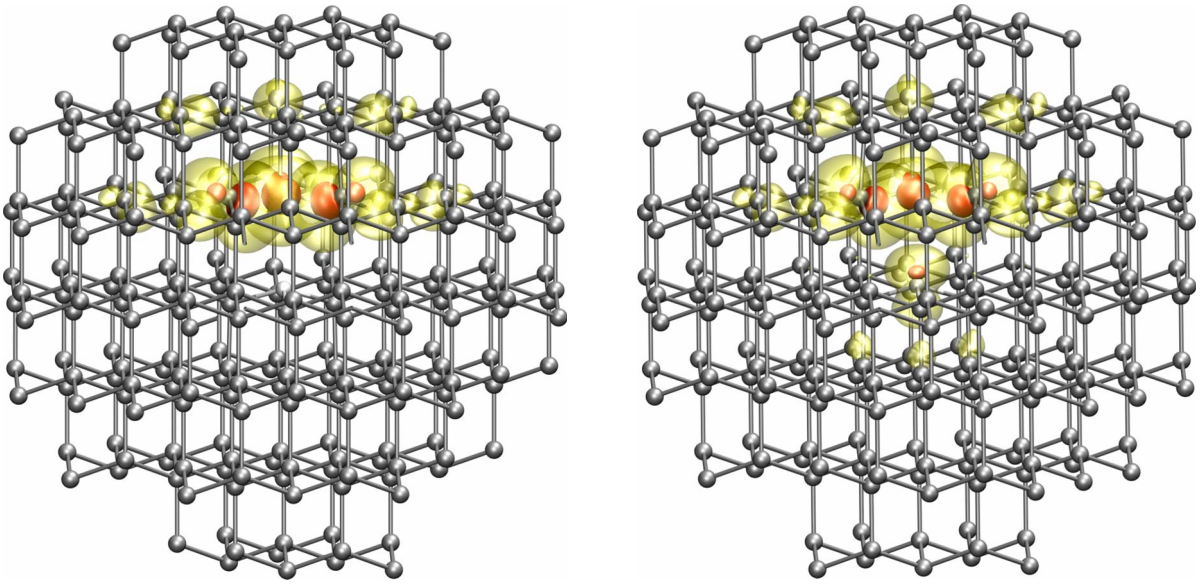

FIG. 1. (Color online) Calculated spin-density isosurfaces. Left panel: ground state ($M_S=\frac{1}{2}$ of ^2E) and right panel: excited state ($M_S=\frac{3}{2}$ of $^4A_2$). Nitrogen and carbon atoms are depicted by very light gray and dark gray balls, respectively. We show two values of spin-density isosurfaces in the left panel: opaque red(dark gray) shows 0.128 (high spin density) while transparent yellow(light gray) shows 0.006 (very small spin density). Right panel shows normalized values in order to show the same effective magnetization density on the atoms as for $S=\frac{1}{2}$ state. The atoms are shown within the radius of 7.3 Å around the nitrogen-atom cut from the 512-atom supercell. The spin density is negligible outside this region. Note that no spin density can be found on nitrogen atom in the ground state while sizeable spin density is localized on nitrogen atom in the excited state. The lobes at the nitrogen and carbon atoms near the vacant site may also represent the corresponding σ_4 and σ_{1-3} dangling bonds in Eq. (1).

barrier is low between the equivalent C_{1h} configurations. Davies concluded from very careful PL studies and analysis that the Jahn-Teller energy of the system should be around 0.14 ± 0.07 eV that is very close to our rough LSDA estimate, 0.09 eV. This result shows clearly a multivalley potential surface for the ground state of this defect as was already hinted by Davies.[32] There may exist more favorable path between these global minima than through the C_{3v} configuration, so the actual barrier energy could be very low. The vibration of atoms may help to gain that barrier energy and result in a motional average between the three equivalent C_{1h} configurations, showing an effective C_{3v} symmetry. It was speculated[32,21] that the dynamic Jahn-Teller effect is responsible for the missing EPR signal of the ^2E ground state. Our calculations support this assumption.

TABLE I. The distances in Ångström unit between the vacant site and nitrogen and nearest-neighbor carbon atoms in different configurations after geometry optimization by LSDA. Our local-density approximation C-C bond length is 1.53 Å in perfect diamond. There are two(three) equivalent carbon atoms in $C_{1h}(C_{3v})$ symmetry as indicated in the parentheses in the third column. In the last column we give the calculated energy differences between these configurations in eV unit. We choose zero energy as a reference for the lowest-energy configuration.

State	Symmetry	Atom	Distance	ΔE
$S=\frac{1}{2}$ A'	C_{1h}	N	1.669	0.00
		C(2×)	1.632	
		C	1.578	
$S=\frac{1}{2}$ ^2E	C_{3v}	N	1.671	0.09
		C(3×)	1.620	
$S=\frac{3}{2}$ $^4A_2$	C_{3v}	N	1.625	0.86
		C(3×)	1.661	

We also investigated the $^4A_2$ excited state. This state has indeed much higher energy by about 0.86 eV compared to that of the low-symmetry ground state. We note that the LSDA total energy differences should not be directly compared to the measured transition energies as previously discussed in Ref. 27. We expect that due to the possibly strong CI correlation between the ^2E ground and excited states, the total energy difference between ^2E ground state and $^4A_2$ excited state is larger than the LSDA value. In the $^4A_2$ excited state the $a_1(2)$ defect level is polarized, thus the nitrogen atom is polarized in contrast to ^2E state (see Fig. 1). This results in considerable rearrangement of the atoms around the vacancy, namely, the nitrogen moves closer to the vacant site (see Table I). We calculated the hyperfine tensors of atoms for the optimum geometry and compared to a recently found EPR center as explained in the introduction[21] (see Table II). The agreement between the calculated and measured hyperfine signal is excellent. The anisotropy in the hyperfine interaction is relatively large which is expected due to the sp^3 character of the dangling bonds. The calculated binding energy of the NV^0 complex ($\approx$3.0 eV) shows a high thermal stability, and its (-/0) occupation level is at about 2.0 eV above valence-band edge, in line with the experimental observations.[19] Thus, we identify the EPR signal of NV^0. We provide the hyperfine data of the three nearest carbon atoms next to the vacant site that has the largest hyperfine interac-

TABLE II. The calculated principal values of the hyperfine tensor (columns 2 to 4) compared to the known experimental data (columns 5 to 7) in MHz for the $^4A_2$ excited state of the *neutral* NV defect. The experimental data on ^{15}N is taken from Ref. 21. The ^{13}C hyperfine signal could not be resolved in that experiment.

Atom	A_{11}	A_{22}	A_{33}	A_{11}^{exp}	A_{22}^{exp}	A_{33}^{exp}
^{15}N	−23.4	−23.4	−39.0	−23.8(3)	−23.8(3)	−35.7(3)
^{13}C(3×)	60.6	61.0	126.2			

tion. These carbon atoms may be measured by future EPR experiments when the signal-to-noise ratio can be reduced there.

V. DISCUSSION OF POSSIBLE SPINTRONICS APPLICATION

After identification of NV^0 defect we discuss its possible role in spin physics. NV^- was successfully used to realize qubits.[9,10] Second-order correlation and EPR measurements were employed to detect individual NV^-. The resulting spin-echo signals show a rapidly oscillating function enveloped by a more slowly oscillating function.[9] The authors of Ref. 9 proposed a theory to explain this signal and they concluded that the fast modulation frequency is due to the effective magnetization density of the electron spin felt by the ^{13}C nucleus, which is the same as the hyperfine interaction. If too many ^{13}C nuclei are involved in the process that will lead to fast decoherence of the spin-echo signal,[9] therefore, the knowledge of the spin-density distribution is crucial. The situation is complex for the ground state as was discussed above. At the measurement temperature an effective C_{3v} symmetry may be detected as the motional average of the three equivalent C_{1h} configurations. It is difficult to handle this situation by quasistatic simulation. We simulate this average simply by taking the optimum ^2E ground state within C_{3v} symmetry. We found that the overall picture is very similar to what was found for NV^-.[27] In the ground state the spin density is mainly localized on the three nearest-neighbor carbon atom of the vacant site and the spin density decays fast as a function of the distance from the vacant site (see Fig. 1). From this point of view, a potential qubit of NV^0 would be weakly coupled to its environment and, therefore, it might present the right coherence properties such as NV^-.

However, the localized spin density is not the only requirement to produce qubits. One needs to generate a superposition state and readout the qubit states. In the case of NV^- the $M_S=0$ of the triplet *ground state* can be optically pumped which has much smaller hyperfine interaction with the proximal ^{13}C nucleus than the $M_S=1$ state.[9] This effect was responsible for the collapse and revival of the electron-spin coherent state. The M_S states could be readout also optically after the measurements by using the fact that they have different fluorescence rates.[9]

In NV^0 defect the optical pump can change the $S=\frac{1}{2}$ state to $S=\frac{3}{2}$ *excited state* and by switching off the light excitation this can be transformed back to the $S=\frac{1}{2}$ state. The nature of the spin-flip process will be discussed shortly. The group-theory analysis tells us that no spin-orbit coupling arises for the $^4A_2$ excited state. However, the spin-spin interaction is active, which can be given by the following effective spin Hamiltonian for this particular system: $\hat{H}_{SS}=D'(S_z^2-5/4)$, where D' is the zero-field constant and S_z has the M_S eigenvalue. (We chose the usual z direction for quantization axis for the spins.) So, the $4\times$ degenerate $^4A_2$ state will split to two double-degenerate states due to spin-spin interaction resulting in the lower lying $M_S=1/2;-1/2$ and the upper lying $M_S=3/2;-3/2$ levels (see Fig. 2). These levels are separated by $2\times D'=D$. $D\approx 1685$ MHz was experimentally measured by EPR.[21] Acording to Davies PL analysis[32] ~2.2 eV excitation occurs between ^2E ground state to the $^2A_1$ excited state. We propose that the $M_S=1/2;-1/2$ electron states of the $^2A_1$ excited state can relax to the $M_S=1/2;-1/2$ sublevels of $^4A_2$ state with a finite probability instead of relaxing back to the ground state. While the spin-orbit interaction is not active for $^2A_1$ state itself the *axial spin-orbit interaction couples the* $^2A_1$ states selectively with the $M_S=1/2;-1/2$ $^4A_2$ *states*. That is the source of the spin-flip process which may be further mediated by phonons in order to satisfy the energy conservation of this transition. Indeed, the threshold excitation energy of the EPR signal, 2.2(1) eV,[21] is larger than the zero-phonon line energy of 2.156 eV and it has the highest intensity using excitation energy of about 2.5 eV. The probability of the relaxation process between the original ^2E and $^1A_1(S=\frac{1}{2})$ states should be higher than for the original $^4A_2(S=\frac{3}{2})$ state. One may estimate from the known data of the NV^- center[34] that the duration of the direct-transition process is about 10 ns, while for the spin-flip process it could be about 30 ns. Therefore, the duration of the optical pumping can be relatively long in order to arrive at $M_S=1/2;-1/2$ sublevels of $^4A_2$ state from the ^2E ground state. The typical EPR condition for $^4A_2$ state is shown in Fig. 2. The small external constant magnetic field (**B**) will split the $M_S=1/2;-1/2$ sublevels lowering the energy of $M_S=-1/2$ state. Finally, we predict that during the optical pumping the $M_S=1/2;-1/2$ sublevels of $^4A_2$ state will be *selectively* populated with somewhat higher probability for $M_S=-1/2$ because it is lower in energy. Then, the varying microwave magnetic field induce the transitions $M_S=\pm 1/2\leftrightarrow\pm 3/2$ in the EPR measurements. This scenario can explain all the photo-EPR findings in Ref. 21.

The question arises what kind of entity can be used as a qubit from NV^0 defect. The first choice is to use simply the S state. By optical pumping the S state of NV^0 defect can be transformed from 1/2 to 3/2 and by switching off the light it can be transformed back from 3/2 to 1/2 with $t\ll 1$ s.[21] However, it may not be probable that coherent state can be

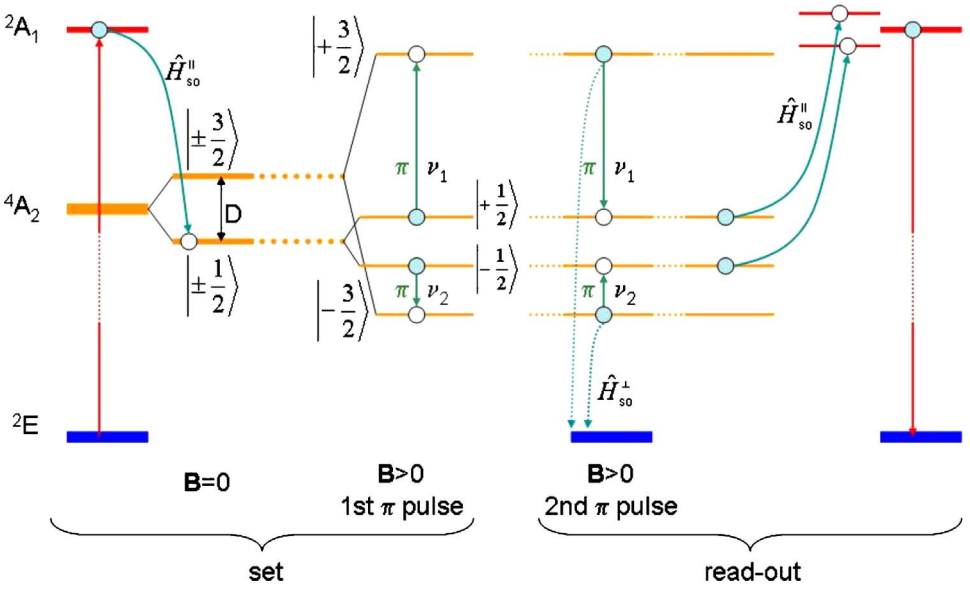

FIG. 2. (Color online) The process of the manipulation of a qubit in NV^0 defect. Straight red(dark gray) arrow dotted in the middle: radiative recombination. Curved green(lighter gray) arrow: spin-orbit coupling ($\hat{H}_{SO}$) possibly mediated by phonons. Light gray dotted arrows represent very weak interaction. Blue(dark gray) straight line: microwave-alternating magnetic-field pulse. Filled(empty) circle: initial(final) state of the electron. Setting the qubit state: (i) excitation from the ^2E ground state to the $^2A_1$ excited state, (ii) spin flip to the appropriate $^4A_2$ states iii) setting either $M_S=3/2$ or $M_S=-3/2$ state by π pulse. Readout the qubit state: i) π pulse to go back to $M_S=\pm 1/2$ states ii) spin flip to the $^2A_1$ state, and (iii) radiative recombination to the ^2E ground state. We show the fine structure of $^4A_2$ states in the absence of external magnetic field ($\mathbf{B}=0$) (2nd column) and at $\mathbf{B}>0$ with typical EPR conditions in the next columns. $D\approx 1685$ MHz fine-structure constant was determined by EPR (Ref. 21). The figure does not show the true scale for the sake of clarity.

achieved for the ground state as our LSDA results indicate that it exhibits a dynamic Jahn-Teller effect causing a *rapidly varying effective magnetic field* for the ^{13}C nuclei around the NV^0 defect. Furthermore, the time-averaged effective hyperfine interaction of both states is very similar (see Fig. 1). This is also disadvantageous.

Another possibility is to use the M_S sublevels of the $^4A_2$ state as qubit. As explained above by optical pumping one can select the $M_S=1/2;-1/2$ sublevels of $^4A_2$ state of the NV^0 defect with *almost equal* probability. That is not applicable for qubits. However, one can selectively set either $M_S=+3/2$ (with energy of $h\nu_1$) or $M_S=-3/2$ ($h\nu_2$) states by applying a π pulse[9] to induce the EPR transition ($\Delta M_S=\pm 1$) (see Fig. 2). *The* $M_S=\pm 3/2$ states may be used as qubit. It is clear in the above mentioned scenario that ν_1 can *only* be associated with $M_S=+3/2$ while ν_2 *only* with $M_S=-3/2$. We would like to emphasize that these metastable $M_S=\pm 3/2$ states are extremely long living (>1 μs) because (i) the $^4A_2$ state is the only $S=3/2$ state, so there is no way for radiative recombination for this state and (ii) the $M_S=\pm 3/2$ states are *not coupled to the* $^2A_1$ excited state at all that hinders the recombination of these states to the ^2E ground state via $^2A_1$ excited state. This is unique compared to the NV^- center[34] and suggests a longer lifetime of these metastable states than for the measured lifetime of the singlet metastable state in NV^- center (300 ns).[34] We note that the $M_S=\pm 3/2$ states are very weakly coupled to the ^2E ground state by *nonaxial* spin-orbit interaction. However, the *nonaxial* spin-orbit interaction is very small (as assumed for NV^- center[34]) and *it is too far in energy in order to mediate this process by phonons*. So, the probability of this decay is very small ensuring the very long lifetime of these states. The coherent state between these $M_S=\pm 3/2$ states and the proximate ^{13}C nuclei can certainly be maintained similar to NV^-.[9] The readout process could be very simple: by applying a π pulse again the $M_S=\pm 3/2$ states scatter to $^4A_2$ $M_S=\pm 1/2$ states that through the spin-orbit coupling can go back to the $^2A_1$ excited state, finally by radiative recombination to the ^2E ground state. Therefore, the spin qubit state can be readout optically. This process can be tuned by applying the appropriate constant magnetic field to split the levels and the microwave magnetic field (π pulse) to induce transitions between the levels.

We mention here that NV^0 defect can have additional advantage over NV^- defect. Recently, NV^--contained nanodiamonds have been demonstrated to act as ultrasensitive magnetometers using different strategies.[22,23] In both cases the sensitivity is proportional to the electron spin state, therefore, the $S=3/2$ excited state of the NV^0 defect would suggest an even more sensitive magnetometer than NV^- defect with $S=1$ state.

VI. SUMMARY AND CONCLUSIONS

In this work we investigated the *neutral* nitrogen-vacancy defect in diamond in detail by *ab initio* LSDA supercell calculations. We showed that the defect indeed shows the dynamic Jahn-Teller effect for the ground state. We identified the recently found EPR center,[21] as the $^4A_2$ excited state of the *neutral* nitrogen-vacancy defect. That EPR center can be used to trace the NV^0-contained nanodiamonds magnetically.

We found that NV^0 is a promising candidate for realizing qubits in diamond *without the need of nitrogen donors*. We propose that NV^0 defect could be an even more sensitive magnetometer than the ultrasensitive NV^- defect.

ACKNOWLEDGMENTS

A.G. acknowledges support from Hungarian OTKA under Contract No. K-67886. The fruitful discussion with Jeronimo Maze is appreciated.

[1] L. du Preez, Ph.D. dissertation, University of Witwatersrand, 1965.
[2] G. Davies and M. F. Hamer, Proc. R. Soc. London, Ser. A **348**, 285 (1976).
[3] J. Wrachtrup, S. Y. Kilin, and A. P. Nizotsev, Opt. Spectrosc. **91**, 429 (2001).
[4] F. Jelezko, I. Popa, A. Gruber, C. Tietz, J. Wrachtrup, A. Nizovtsev, and S. Kilin, Appl. Phys. Lett. **81**, 2160 (2002).
[5] F. Jelezko, T. Gaebel, I. Popa, A. Gruber, and J. Wrachtrup, Phys. Rev. Lett. **92**, 076401 (2004).
[6] F. Jelezko, T. Gaebel, I. Popa, M. Domhan, A. Gruber, and J. Wrachtrup, Phys. Rev. Lett. **93**, 130501 (2004).
[7] R. J. Epstein, F. Mendoza, Y. K. Kato, and D. D. Awschalom, Nat. Phys. **1**, 94 (2005).
[8] R. Hanson, F. M. Mendoza, R. J. Epstein, and D. D. Awschalom, Phys. Rev. Lett. **97**, 087601 (2006).
[9] L. Childress, M. V. Gurudev Dutt, J. M. Taylor, A. S. Zibrov, F. Jelezko, J. Wrachtrup, P. R. Hemmer, and M. D. Lukin, Science **314**, 281 (2006).
[10] M. V. Gurudev Dutt, L. Childress, L. Jiang, E. Togan, J. Maze, F. Jelezko, A. S. Zibrov, P. R. Hemmer, and M. D. Lukin, Science **316**, 1312 (2007).
[11] R. Hanson, V. V. Dobrovitski, A. E. Feiguin, O. Gywat, and D. D. Awschalom, Science **320**, 352 (2008).
[12] J. H. N. Loubser and J. P. van Wyk, *Diamond Research (London)* (Industrial Diamond information Bureau, London, 1977), pp. 11–15.
[13] R. Hanson, O. Gywat, and D. D. Awschalom, Phys. Rev. B **74**, 161203(R) (2006).
[14] S. Takahashi, R. Hanson, J. van Tol, M. S. Sherwin, and D. D. Awschalom, Phys. Rev. Lett. **101**, 047601 (2008).
[15] S.-J. Yu, M.-W. Kang, H.-C. Chang, K.-M. Chen, and Y.-C. Yu, J. Am. Chem. Soc. **127**, 17604 (2005).
[16] Y.-R. Chang, H.-Y. Lee, K. Chen, C.-C. Chang, D.-S. Tsai, C.-C. Fu, T.-S. Lim, Y.-K. Tzeng, C.-Y. Fang, C.-C. Han, H.-C. Chang, and W. Fann, Nat. Nanotechnol. **3**, 284 (2008).
[17] J. Rabeau, A. Stacey, A. Rabeau, S. Prawer, F. Jelezko, I. Mirza, and J. Wrachtrup, Nano Lett. **7**, 3433 (2007).
[18] G. Davies, S. C. Lawson, A. T. Collins, A. Mainwood, and S. J. Sharp, Phys. Rev. B **46**, 13157 (1992).
[19] Y. Mita, Phys. Rev. B **53**, 11360 (1996).
[20] T. A. Kennedy, J. S. Colton, J. E. Butler, R. C. Linares, and P. J. Doering, Appl. Phys. Lett. **83**, 4190 (2003).
[21] S. Felton, A. M. Edmonds, M. E. Newton, P. M. Martineau, D. Fisher, and D. J. Twitchen, Phys. Rev. B **77**, 081201(R) (2008).
[22] J. R. Maze, P. L. Stanwix, J. S. Hodges, S. Hong, J. M. Taylor, P. Capallero, L. Jiang, M. V. G. Dutt, E. Dogan, A. S. Zibrov, A. Yacobi, R. L. Walsworth, and M. D. Lukin, Nature (London) **455**, 644 (2008).
[23] G. Balasubramanian, I. Y. Chan, R. Kolesov, M. Al-Hmoud, J. Tisler, C. Shin, C. Kim, A. Wojcik, P. R. Hemmer, A. Krueger, T. Hanke, A. Leitenstorfer, R. Bratschitsch, F. Jelezko, and J. Wrachtrup, Nature (London) **455**, 648 (2008).
[24] G. Kresse and J. Furthmüller, Phys. Rev. B **54**, 11169 (1996).
[25] P. E. Blöchl, C. J. Först, and J. Schimpl, Bull. Mater. Sci. **26**, 33 (2003).
[26] P. E. Blöchl, Phys. Rev. B **50**, 17953 (1994).
[27] A. Gali, M. Fyta, and E. Kaxiras, Phys. Rev. B **77**, 155206 (2008).
[28] S. Felton, A. M. Edmonds, M. E. Newton, P. M. Martineau, D. Fisher, D. J. Twitchen, and J. M. Baker, Phys. Rev. B **79**, 075203 (2009).
[29] A. Lenef and S. C. Rand, Phys. Rev. B **53**, 13441 (1996).
[30] J. A. Larsson and P. Delaney, Phys. Rev. B **77**, 165201 (2008).
[31] J. P. Goss, R. Jones, S. J. Breuer, P. R. Briddon, and S. Öberg, Phys. Rev. Lett. **77**, 3041 (1996).
[32] G. Davies, J. Phys. C **12**, 2551 (1979).
[33] A. S. Zyubin, A. M. Mebel, M. Hayashi, H. C. Chang, and S. H. Lin, J. Comput. Chem. **30**, 119 (2009).
[34] N. B. Manson, J. P. Harrison, and M. J. Sellars, Phys. Rev. B **74**, 104303 (2006).